Experimental Thermal Validation of Two Vector Potential Formulations in Industrial Transverse Flux Induction Heating Process

Catherine Guarneri, Philippe Massé, Yves du Terrail
MADYLAM, ENSHMG, B.P. 95
38402 Saint Martin d'Hères, FRANCE

Abstract **-- A 3D package has been developed to compute the transverse flux induction heating of flat products. It contains two vector potential formulations of the electromagnetic equations and a thermal equation. All these 3D equations are solved by F.E.M.. Numerical results are compared to experimental measurements on an industrial-scale prototype.**

I. INTRODUCTION

A transverse flux induction heating device is an electromagnetic device with a travelling load at constant velocity, where magneto-dynamic and heat transfer phenomena occur. Transverse flux induction is used to heat very thin strips of non-magnetic conductive material, such as aluminium. The source currents induce eddy currents which heat the strip by Joule's effect (Fig. 1). Resultant heating is uniform except on the load borders, where under-heating (or over-heating) can occur as the strip is larger (or narrower) than the inductor (Fig. 2).

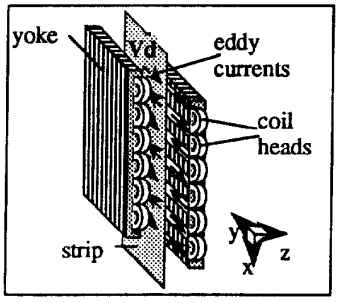

Fig. 1. Transverse flux induction heating device.

An industrial-scale prototype of inductor has been built at MADYLAM laboratory. The device is one meter high and is placed vertically. A five-meter high frame supports the inductors and the rollers which maintain the strip in place (Fig. 3). As it can be seen in Fig. 1 and Fig. 2, transverse flux induction heating devices have a true tridimensional geometry. For this reason, in order to compute transverse flux induction heating, a 3D F.E. package has been made that would be of great help to the designer.

The numerical results of this package have been compared to the experimental measurements made on the MADYLAM prototype. The measurements which were carried out lead to:

- a map of the 3 components of the induction field $\vec{B}$ in the air gap between the strip and one half of the inductor (Fig. 4),
- a map of the temperature on the strip travelling into the inductor (Fig. 5).

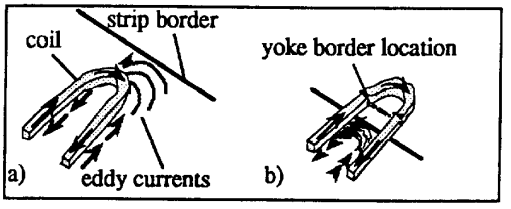

Fig. 2. The drawing of eddy current lines
a) The strip is larger than the inductor, including coil heads.
b) The strip is narrower than the yoke of the inductor.

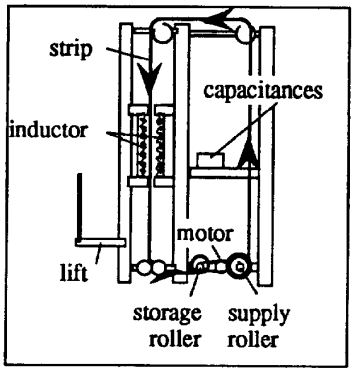

Fig. 3. General view of the structure showing how the strip and the inductor are held in place.

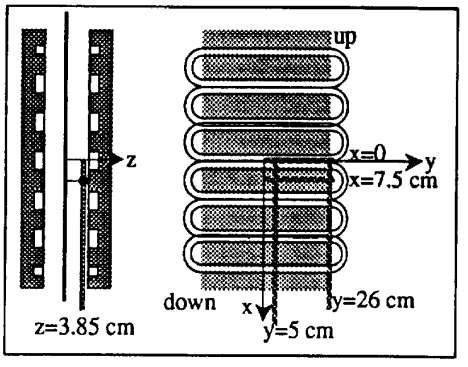

Fig. 4. Induction field measurements location.

Manuscript received July 6th, 1994. This work was supported in part by Electricité De France, centre des Renardières.

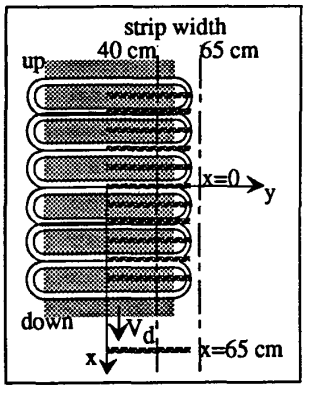

Fig. 5. Strip temperature measurements location.

Fig. 6 shows a good agreement between computed and experimental induction fields [1], in the case of an aluminium strip, which receives 5.27 kW power density at 1050 Hz working frequency, with an inductor gap of 10 cm wide.

This paper presents, at first, the 3D F.E. package and then the experimental thermal validition of the numerical modelling.

II. The 3D finite element package

The electromagnetic field and thermal coupled problems have been taken into account. Two formulations for the electromagnetic equations have been used : one with the modified vector potential $\vec{A}^*$ and the other with $(\vec{A},v)$, where $\vec{A}$ is the vector potential and the scalar potential Φ is a time derivative of v [2], the gauge is Coulomb's. Complex numbers are used for time treatment. Laplace eddy currents, $\sigma \vec{V} \times \vec{B}$ are neglected, where σ is the electrical conductivity.

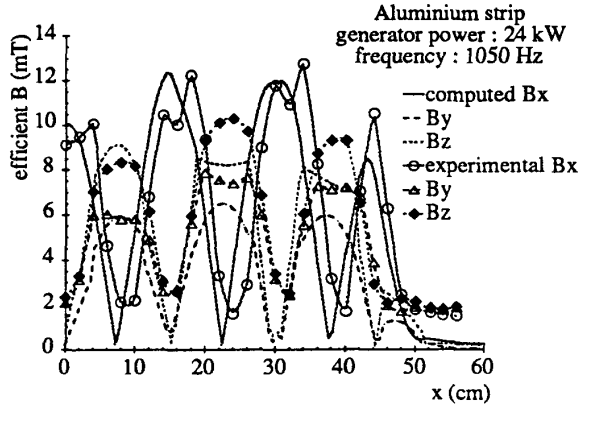

Fig. 6. Induction field along the vertical facing the coil heads.

The heat transfer equation, with a travelling load at constant velocity $\vec{V}$, expresses the steady state in the inductor referential. The thermal power density in the load proceeds from Joule's losses. Since the electromagnetic properties are not strongly temperature dependent in the studied process, it is not necessary to solve the two equations simultaneously. From the solution of the electromagnetic equation, the thermal power density can be deduced. Then, solving the heat transfer equation, gives the temperature map in the strip. Both equations have been solved with nodal elements and 2nd order Lagrange polynomials as shape functions. The package has been realised with FLUX EXPERT [3].

It is well known that nodal elements with second order Lagrange polynomials do not insure the conservation of eddy currents in the modified vector potential formulation, even if the condition $\mathrm{div}\,\vec{A}^* = 0$ is imposed by penalization in the induction equation [4]. Eddy currents are better conserved by $(\vec{A},v)$ formulation than by a $\vec{A}^*$ formulation.

The variational formulation for the modified vector potential equation is:

$$\int_\Omega \upsilon_r \vec{\mathrm{curl}}\vec{A}^*.\vec{\mathrm{curl}}\vec{W}\,d\Omega+\int_\Omega \upsilon_p \mathrm{div}(\vec{A}^*).\mathrm{div}(\vec{W})\,d\Omega$$
$$+\int_\Omega j\omega\sigma\mu_0\vec{A}^*.\vec{W}\,d\Omega=\int_\Omega \mu_0\vec{J}_{ex}.\vec{W}\,d\Omega$$

The variational formulation for $(\vec{A},v)$ equation is :

$$\int_\Omega \upsilon_r \vec{\mathrm{curl}}\vec{A}.\vec{\mathrm{curl}}\vec{W}\,d\Omega+\int_\Omega \upsilon_p \mathrm{div}(\vec{A})\mathrm{div}(\vec{W})\,d\Omega$$
$$+\int_\Omega j\omega\sigma\mu_0\vec{A}.\vec{W}\,d\Omega+\int_\Omega j\omega\sigma\mu_0\vec{\mathrm{grad}}v.\vec{W}\,d\Omega=\int_\Omega \mu_0\vec{J}_{ex}.\vec{W}\,d\Omega$$

and

$$\int_\Omega j\omega\sigma\mu_0\vec{A}.\vec{\mathrm{grad}}v\,w\,d\Omega+\int_\Omega j\omega\sigma\mu_0\vec{\mathrm{grad}}v.\vec{\mathrm{grad}}w\,d\Omega=0$$

The variational formulation for the heat transfer equation is:

$$\int_\Omega \rho C\Theta\vec{V}.\vec{\mathrm{grad}}T\,d\Omega+\int_\Omega k\,\vec{\mathrm{grad}}T.\vec{\mathrm{grad}}\Theta\,d\Omega+\int_\Gamma h(T-T_a)\Theta\,d\Gamma$$
$$+\int_\Gamma \varepsilon\sigma_b(T^4-T_a^4)\,\Theta\,d\Gamma=\int_\Omega \frac{1}{2\sigma}\vec{J}.\vec{J}^c\Theta\,d\Omega$$

Nomenclature

- $\vec{A}^*$: modified vector potential
- $\vec{A},\Phi$: 4 vector potential - scalar and vector -
- v : time primitive of Φ
- $\vec{J}$: eddy currents density
- $\vec{J}_{ex}$: complex electrical source density
- σ : electrical conductivity
- υ_r : relative reluctivity
- υ_p : penalty coefficient
- ω : electrical angular frequency
- j : complex number, $j^2 = -1$

$(.)^c$: conjugate of a complexe number
$\vec{n}$: normal vector
$\vec{W}$: vector basis functions for Galerkin's projection
w : basis functions for Galerkin's projection
T : temperature
T_a : ambient temperature
ρ : volumic mass
C : calorific capacity
k : thermal conductivity
$\vec{V}$: load velocity
θ : basis functions for Galerkin's projection

III. Experimental Thermal Validation

A. Modified vector potential in conductive regions

Using $\vec{A}^*$ to compute eddy currents may seem audacious. However, there are some cases in which the modified vector potential is suitable. The inconvenience of $\vec{A}^*$, when it is used with nodal elements and second order Lagrange polynomials, is that it does not allow normal discontinuity of the electric field $\vec{E}$ at the boundary between regions of different electric conductivities, since $\vec{E} = -j\omega\vec{A}^*$. Therefore, it can be used if there is no problem of discontinuity of $\vec{E}.\vec{n}$. For instance, when the nearby eddy currents are parallel to the boundary between regions of different electric conductivities, or when there are no eddy currents near this boundary, it is judicious to choose the modified vector potential as it leads to only 3 complex components per node, versus 4 with the formulation $(\vec{A},v)$.

Fig. 7 refers to the heating of an aluminium strip which is much larger than the inductor, at a frequency of 300 Hz. It is in good agreement with another numerical simulation where the electric field is computed by a hybrid finite element-boundary integral method. The finite elements are Whitney edge elements and the mesh is made of tetrahedra [5] [6].

Fig. 8 relates the comparison between experimental measurements on the inductor prototype of MADYLAM laboratory, in the case where the aluminium strip is larger than the inductor, at a frequency of 1500 Hz, and numerical results of the two formulations $\vec{A}^*$ and $(\vec{A},v)$ coupled with the thermal problem. Both formulations predict an under-heating on the border of the strip.

These two examples demonstrate that the $\vec{A}^*$ formulation can be used when there are no normal eddy currents near the edge of the strip, and it is worth choosing this formulation in order to save memory.

B. Using $(\vec{A},v)$ formulation

However, when eddy currents come normal to the interface of two regions with different conductivities, the $\vec{A}^*$ formulation should not be used, as it imposes on the electric field, a normal continuity which must not exist. In that case, the $(\vec{A},v)$ formulation has been chosen to simulate transverse

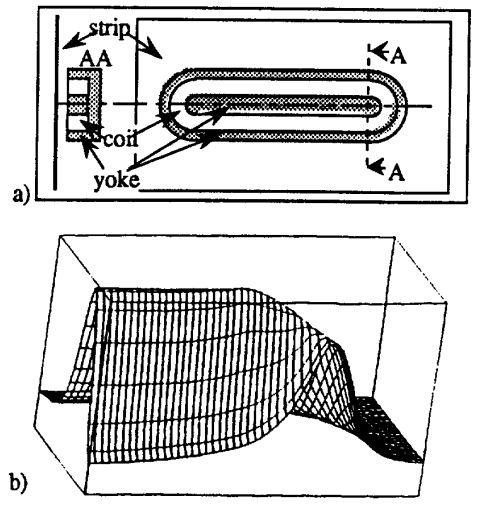

Figure 7 : The strip is much larger than the inductor.
a) Monopole inductor geometry. b) Joule loss density on the strip.

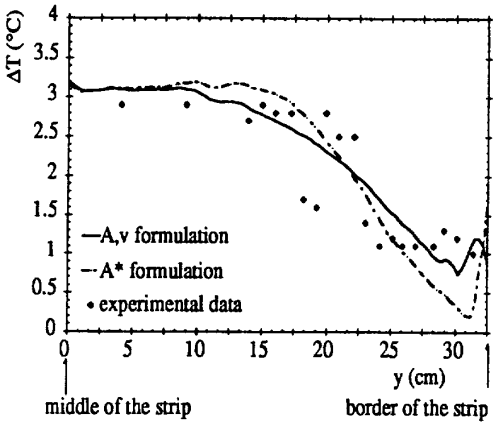

Figure 8 : Rise in temperature when the strip crosses half pole.
The strip is larger than the inductor.

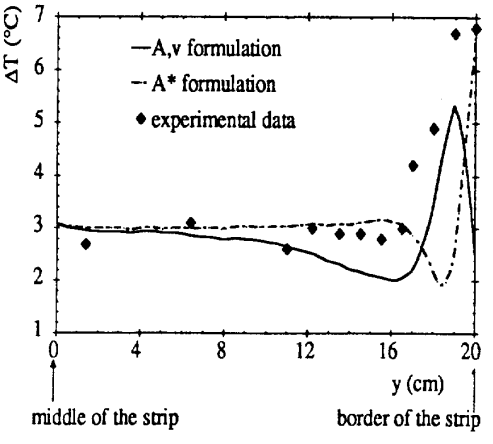

Figure 9 : Rise in temperature when the strip crosses half pole.
The strip is narrower than the inductor.

flux induction heating of strips which are narrower than the inductor. Numerical and experimental results are shown in Fig. 9, with an aluminium strip, at a frequency of 1500 Hz. In spite of a satisfactory agreement, they pointed out a third problem : the existence of bifurcation points.

IV. Bifurcation points

When the strip is narrower than the inductor, the source currents force the eddy currents to follow them, so the eddy currents come normal to the border of the strip. As they can't go out of the strip, they have to corner sharply very close to the border. But they have the choice to turn right or left hand. In fact, the layer of currents divides into two equal parts. As Fig. 10 shows it, point P is singular, it is a bifurcation point. There are bifurcation points on the border of the strip, facing every side of each pole, if the inductor is larger than the load.

Special attention should be paid to computing eddy currents at those points. The current density vector, which is parallel to Oy at node 2, must be parallel to the border (Ox) at node 4. Which direction has this vector on node 3 (Fig. 11) ? The answer to this question should take into account the conservation of the currents, and must avoid a loss of computed power in the neighbourhood of point P, because it is in that region that the tightening of the current lines produces a maximum of thermal power density, which is responsible for the over-heating of the border of the strip.

The problem comes from the strong decrease of the values of the y-component of the eddy current density vector, between nodes 1 and 3, and from the strong increase of its x-component value, between nodes 3 and 5. As thermal power density proceeds from the interpolation of $\vec{J}$ between the electromagnetic mesh and the thermal mesh, those variations produce a numerical loss of power on the border of the strip.

Decreasing the size of the meshes would be a solution. In spite of the use of 22572 unknowns, the problem of the bifurcation point produces numerical oscillation in this area, even with the $(\vec{A},v)$ formulation. The matrix was ill-conditionned for each formulation. Further it is non symmetric for the $\vec{A}^*$ formulation, because it is necessary to impose the condition $\vec{A}^*.\vec{n}=0$ on the boundary between the load and the air gap, to insure the conservation of eddy currents there. This condition is set as a boundary condition and turns out to break the matrix symmetry.

Conclusion

The 3D FE package which is presented in this paper can be useful for designing transverse flux induction heating devices. Two formulations are proposed. The $\vec{A}^*$ formulation is to be used when the normal discontinuity of the electric field is weak at the edge of the load. The $(\vec{A},v)$ formulation will be used for strong discontinuities, that is when the strip is narrower than the inductor. In fact the $(\vec{A},v)$ formulation can be used in every case, but the $\vec{A}^*$ formulation leads to fewer unknowns per node.

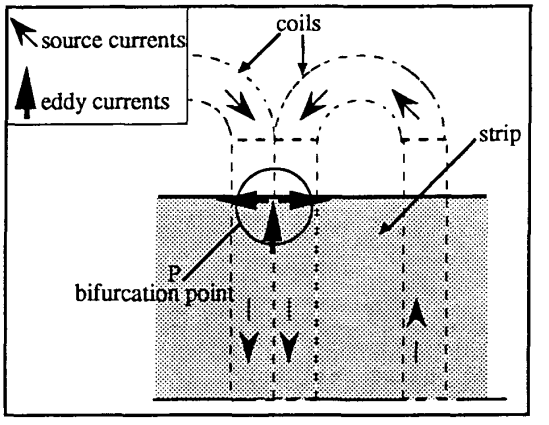

Figure 10 : A bifurcation point

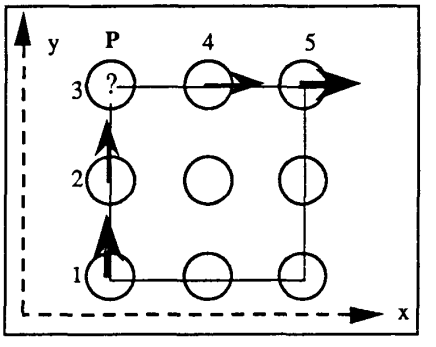

Figure 11 : The eddy current density vector in an element with a point P

REFERENCES

[1] Catherine Guarneri, Yves du Terrail Couvat, Philippe Massé, "3D Modelisations of Transverse Flux Induction Heating Processes, an Experimental Validation", International Workshop on Electric and Magnetic Fields, Liege, Belgium, September 1992.

[2] Oszkar Biro and Kurt Preis, "On the Use of the Magnetic Vector Potential in the Finite Element Analysis of Three-Dimensional Eddy Currents", IEEE Transactions on magnetics, Vol. 25, NO. 4, pp 3145-3159, July 1989.

[3] Ph. Massé, "Modelling of continuous media methodology and CAD of Finite Element Programs," *INTERMAG Conference, Hamburg, F.R.G.*, 1984.

[4] Jean Louis Coulomb, "Analyse tridimensionnelle des champs electriques et magnétiques par la méthode des éléments finis", Thèse d'Etat, Grenoble, June 1981.

[5] J.Y. Bidan, G. Nicolas, "Etude numérique d'un dispostif de chauffage par induction en flux transverse", note E.D.F. HI 72/7533, September 1991.

[6] Z. Ren, F. Bouillault, A. Razek, A. Bossavit, J.C. Vérité, "A new hybrid model usig electric field formulation for 3-D eddy current problems", IEEE Transactions on magnetics, Vol.26, NO. 2, pp 470-473, March 1990.